university of groningen

University Medical Center Groningen

University of Groningen

More Frequent, Intense, and Extensive Rainfall Events in a Strongly Warming Arctic

Dou, T. F.; Pan, S. F.; Bintanja, R.; Xiao, Cunde

Published in:
Earths future

DOI:
10.1029/2021EF002378

IMPORTANT NOTE: You are advised to consult the publisher's version (publisher's PDF) if you wish to cite from it. Please check the document version below.

Document Version
Publisher's PDF, also known as Version of record

Publication date:
2022

Link to publication in University of Groningen/UMCG research database

Citation for published version (APA):
Dou, T. F., Pan, S. F., Bintanja, R., & Xiao, C. (2022). More Frequent, Intense, and Extensive Rainfall Events in a Strongly Warming Arctic. *Earths future*, *10*(10), [ARTN e2021EF002378]. https://doi.org/10.1029/2021EF002378

Copyright
Other than for strictly personal use, it is not permitted to download or to forward/distribute the text or part of it without the consent of the author(s) and/or copyright holder(s), unless the work is under an open content license (like Creative Commons).

The publication may also be distributed here under the terms of Article 25fa of the Dutch Copyright Act, indicated by the “Taverne” license. More information can be found on the University of Groningen website: https://www.rug.nl/library/open-access/self-archiving-pure/taverne-amendment.

Take-down policy
If you believe that this document breaches copyright please contact us providing details, and we will remove access to the work immediately and investigate your claim.

Downloaded from the University of Groningen/UMCG research database (Pure): http://www.rug.nl/research/portal. For technical reasons the number of authors shown on this cover page is limited to 10 maximum.

Download date: 28-12-2022

Check for updates

Earth's Future

RESEARCH ARTICLE
10.1029/2021EF002378

Special Section:
Atmospheric Rivers: Intersection of Weather and Climate

More Frequent, Intense, and Extensive Rainfall Events in a Strongly Warming Arctic

T. F. Dou[1], S. F. Pan[2], R. Bintanja[3,4], and C. D. Xiao[5]

[1]College of Resources and Environment, University of Chinese Academy of Sciences, Beijing, China, [2]Key Laboratory of Meteorological Disaster, Ministry of Education, Nanjing University of Information Science and Technology, Nanjing, China, [3]Royal Netherlands Meteorological Institute (KNMI), De Bilt, The Netherlands, [4]Energy and Sustainability Research Institute Groningen (ESRIG), University of Groningen, Groningen, The Netherlands, [5]State Key Laboratory of Earth Surface Processes and Resource Ecology, Beijing Normal University, Beijing, China

Abstract The changes in the Arctic precipitation profoundly impact the surface mass balance of ice sheet and sea ice, the extent of snow cover, as well as the land/ice surface runoff in the Arctic, particularly when it occurs in liquid form. Here, we use state-of-the-art models from the Coupled Model Intercomparison Project Phase 5 to project the number of days with rainfall, the intensities and onset dates of rainfall events in the Arctic under the strong emission scenario (RCP8.5). The multi-model mean shows that rainfall will occur more frequently in the Arctic at the end of this century (2091–2100), with larger increase in the rainy days over the Pacific and Atlantic sectors (up to 12 days/month) during the cold seasons (October–May) and over the Arctic Ocean (up to 14 days/month) during the warm seasons (June–September) as compared with the present day (2006–2015). Greater uncertainty is found in the cold seasons, which mainly comes from the high variability among different models in the Norwegian Sea. Sixty-seven to ninety-three percentage of the increases in rainy days is contributed by the local warming and the remainder by the increase in total precipitation. Moreover, at the end of this century, the rainfall in spring will occur much earlier than the present day by more than 1 month, and the extent of rainfall will further expand toward the center of the Arctic Ocean and the inland Greenland in the future. The changes of rainfall intensity on the Arctic land area to the climate warming are more sensitive than that on the Arctic Ocean in warm seasons (May–September). The rainfall will be further strengthened in most of the Arctic continents in summer, with the largest increase in the intensity of ~2 mm/day along the southwest coast of Greenland. The above results are confirmed by the latest projections from CMIP6 models.

Plain Language Summary There is increasing interest in the response of the Arctic precipitation, especially for its liquid form, to changing climate because of their great impacts on land/ice surface runoff and the freezing and thawing processes of snow and ice. However, the spatiotemporal distribution and future changes in the frequency, timing, and intensity of rainfall events in the Arctic are poorly understood. This study reveals that the increase in rainfall in the Arctic is reflected not only in frequency but also in intensity and range. The rainfall will further advance toward the center of the Arctic Ocean and the inland area of Greenland at the end of this century, leading to more and more rainfall events in these areas. Meanwhile, the timing of rainfall in spring will be significantly advanced, taking the Chukchi Sea and the Northern Barents Sea as an example; the first spring rainfall in these areas at the end of this century will occur 3 months earlier than the present-day. All these trends will make rainfall a new force, accelerating the melting of snow and ice in the Arctic in the future. We further found that local warming is the main reason for more rainfall days in the Arctic. Actually, it determines almost all the increases on rainy days in the areas where precipitation phase change is highly sensitive to the temperature rise.

Key Points:

- The increase of the Arctic rainfall in the future performs not only in the increase in the frequency but also the intensity
- Arctic rainfall events in spring will occur much earlier at the end of this century
- The extent of rainfall will further expand toward the center of the Arctic Ocean and the inland Greenland in the future

Supporting Information:

Supporting Information may be found in the online version of this article.

Correspondence to:

C. D. Xiao,
cdxiao@bnu.edu.cn

Citation:

Dou, T. F., Pan, S. F., Bintanja, R., & Xiao, C. D. (2022). More frequent, intense, and extensive rainfall events in a strongly warming Arctic. *Earth's Future*, *10*, e2021EF002378. https://doi.org/10.1029/2021EF002378

Received 29 AUG 2021
Accepted 13 SEP 2022

© 2022 The Authors. Earth's Future published by Wiley Periodicals LLC on behalf of American Geophysical Union. This is an open access article under the terms of the Creative Commons Attribution-NonCommercial-NoDerivs License, which permits use and distribution in any medium, provided the original work is properly cited, the use is non-commercial and no modifications or adaptations are made.

1. Introduction

The response of Arctic precipitation to climate warming is much more sensitive than that of global mean precipitation (Bintanja & Selten, 2014; Boer, 2009; Trenberth, 2011), mainly due to the enhanced local surface evaporation associated with the sea ice retreat (Bintanja et al., 2020). A rapid increase in Arctic precipitation can regulate the regional hydrological cycle, impacting greatly the evolution of the ecological system (Vihma et al., 2016; Wrona et al., 2016; Zhang et al., 2013). The changes in amount and phase of precipitation affect the freeze-thaw process of snow and sea ice (e.g., Dou et al., 2019; Perovich et al., 2017; Screen & Simmond, 2012)

23284277, 2022, 10, Downloaded from https://agupubs.onlinelibrary.wiley.com/doi/10.1029/2021EF002378 by Universitetsbiblioteket, Wiley Online Library on [17/11/2022]. See the Terms and Conditions (https://onlinelibrary.wiley.com/terms-and-conditions) on Wiley Online Library for rules of use; OA articles are governed by the applicable Creative Commons License

23284277, 2022, 10, Downloaded from https://agupubs.onlinelibrary.wiley.com/doi/10.1029/2021EF002378 by Universitetsbiblioteket, Wiley Online Library on [17/11/2022]. See the Terms and Conditions (https://onlinelibrary.wiley.com/terms-and-conditions) on Wiley Online Library for rules of use; OA articles are governed by the applicable Creative Commons License

and the surface mass balance of the Greenland Ice Sheet (Bring et al., 2016; Oltmanns et al., 2019; Shepherd et al., 2019). The increase in precipitation can desalinate the Arctic Ocean and subsequently modulate the Atlantic meridional overturning circulation (Davies et al., 2014; Kattsov & Walsh, 2000).

In addition to the amount of precipitation, other precipitation variables, such as frequency and intensity, also play an important role in regional climate change (Trenberth et al., 2003) by modulating soil moisture, evaporation, and surface heat flux (Perovich et al., 2017; Qian et al., 2006; Trenberth, 2011). For example, for the same amount of precipitation in the same period, a few times of heavy precipitation events have much more serious negative impacts on the survival of Arctic aborigines and local infrastructure than many times of mild precipitation events (e.g., Forbes et al., 2016; Vihma et al., 2016). Moreover, the frequency and intensity of precipitation can be used to validate the cloud physical parameterization in weather and climate models (e.g., Lopez, 2007). However, few studies have focused on the frequency and intensity of precipitation in the Arctic (Cohen et al., 2015), and little is known about their changes in the Arctic Basin, and the projections have not yet been conducted.

This study aims to project the number of days with precipitation as well as the intensity and timing of the precipitation over the Arctic, and mainly focuses on rainfall events, since it is believed that liquid will be the dominant phase of precipitation in the Arctic in the future (Bintanja & Andry, 2017; Pan et al., 2020). First, we used the ERA5, ERA-Interim, and MERRA reanalysis data sets to validate the multi-model mean results for the present-day climate. Then, we quantified the seasonal cycle of rainy days, the onset dates and the intensity of rainfall for the future climate (2091–2100). The projections were performed by the Coupled Model Intercomparison Project Phase 5 (CMIP5) models under the strong emission scenario (RCP8.5), and the trends at the end of this century were specified by comparing with the current climate (2006–2015). Furthermore, we estimated the contribution of local warming to the increase in rainy days. Finally, we use the simulations of the latest phase of CMIP (CMIP6) models to verify the results derived from the CMIP5 models.

2. Materials and Methods

The model output data used in this study are an integral part of the CMIP5 models and the latest phase (CMIP6) initiative. All data for the CMIP5 models are publicly available at http://cmip-pcmdi.llnl.gov/cmip5 and the outputs of the CMIP6 models are available at https://esgf-node.llnl.gov/search/cmip6/. Daily outputs from the CMIP5 model were used for simulations with the RCP8.5 scenario for the period of 2006–2100. The CMIP6 projections with the high-emission scenario (SSP585) in 2015–2100 were used to validate the results derived from the CMIP5 models during the same period. First, we selected the models from all available CMIP5 models for which data coverage was complete and without obvious errors and for which daily fields of air temperature, total precipitation and snowfall were available. In total, 21 CMIP5 (r1i1p1) models were used (Table 1). For CMIP6, 11 CMIP6 (r1i1p1f1) models were applied in this study (Table 2). The multimodel mean was evaluated to characterize the "best estimate" of the simulations conducted with the CMIP model ensembles.

Before conducting the projections, we took the reanalysis data as the true value to correct the simulations of each model. Specifically, the ratio of reanalysis and model data of daily precipitation was used as a correction factor, which was computed monthly at each grid point, to multiply the original model output to yield the final precipitation data. The ERA5 reanalysis was used for the corrections of total precipitation and rain, and ERA-Interim was used for the correction of date of first rainfall, since they have obvious advantages in depicting different precipitation phases and rainfall timing in the Arctic (Dou et al., 2021). Then, these corrected data were used to calculate the multi-model mean values. The rainy days, for instance, were computed in each ensemble member individually and then used to calculate the average value. The reanalysis data sets (ERA-Interim, ERA5, and MERRA) are publicly available through their respective web portals (see "Data Availability Statement" section). The data of total precipitation and snowfall were used in this study, and the amount of rainfall was derived from their difference. The reanalysis data were used to verify the CMIP5 multi-model mean results during the present-day period of 2006–2015. All the model and reanalysis data were interpolated to a resolution of $0.5° \times 0.5°$ using bilinear interpolation.

This study mainly focuses on the following precipitation-related variables: precipitation (rainfall) intensity, maximum precipitation (rainfall) intensity, number of days with precipitation (rainfall), and dates of first rainfall events. Precipitation (rainfall) events were determined using 1.0 mm day^{-1} as a threshold. We repeated the analysis with various thresholds, and the threshold of 1.0 mm day^{-1} did not materially alter the results and had the

23284277, 2022, 10, Downloaded from https://agupubs.onlinelibrary.wiley.com/doi/10.1029/2021EF002378 by Universiteitsbibliotheek, Wiley Online Library on [17/11/2022]. See the Terms and Conditions (https://onlinelibrary.wiley.com/terms-and-conditions) on Wiley Online Library for rules of use; OA articles are governed by the applicable Creative Commons License

Table 1
Description of the Coupled Model Intercomparison Project Phase 5 Models (21 in Total) Used in the Study

Model	Institution	Grid points (latitude × longitude)
ACCESS1-0	Centre for Australian Weather and Climate Research (Australia)	145 × 192
ACCESS1-3	Centre for Australian Weather and Climate Research (Australia)	145 × 192
CanESM2	Canadian Centre for Climate Modelling and Analysis (Canada)	64 × 128
CMCC-CESM	Centro Euro-Mediterraneo per I Cambiamenti Climatici (Italy)	48 × 96
CMCC-CMS	Centro Euro-Mediterraneo per I Cambiamenti Climatici (Italy)	96 × 192
CNRM-CM5	Centre National de Recherches Meteorologiques/Centre Europeen de Recherche et Formation Avancees en Calcul Scientifique (France)	128 × 256
CSIRO-Mk3-6-0	Commonwealth Scientific and Industrial Research Organization/Queensland Climate Change Centre of Excellence (Australia)	96 × 192
FGOALS-s2	LASG, Institute of Atmospheric Physics, Chinese Academy of Sciences (China)	108 × 128
GFDL-CM3	Geophysical Fluid Dynamics Laboratory (United States)	90 × 144
GFDL-ESM2G	Geophysical Fluid Dynamics Laboratory (United States)	90 × 144
GFDL-ESM2M	Geophysical Fluid Dynamics Laboratory (United States)	90 × 144
IPSL-CM5A-LR	Institut Pierre Simon Laplace (France)	96 × 96
IPSL-CM5A-MR	Institut Pierre Simon Laplace (France)	143 × 144
IPSL-CM5B-LR	Institut Pierre Simon Laplace (France)	96 × 96
MIROC5	Atmosphere and Ocean Research Institute (The University of Tokyo), National Institute for Environmental Studies, and Japan Agency for Marine-Earth Science and Technology (Japan)	128 × 256
MIROC-ESM	Atmosphere and Ocean Research Institute (The University of Tokyo), National Institute for Environmental Studies, and Japan Agency for Marine-Earth Science and Technology (Japan)	64 × 128
MIROC-ESM-CHEM	Atmosphere and Ocean Research Institute (The University of Tokyo), National Institute for Environmental Studies, and Japan Agency for Marine-Earth Science and Technology (Japan)	64 × 128
MPI-ESM-LR	Max Planck Institute for Meteorology (Germany)	96 × 192
MPI-ESM-MR	Max Planck Institute for Meteorology (Germany)	96 × 192
MRI-CGCM3	Meteorological Research Institute (Japan)	160 × 320
MRI-ESM1	Meteorological Research Institute (Japan)	160 × 320

Table 2
Description of the CMIP6 Models (11 in Total) Used in the Study

Model	Institution	Grid points (latitude × longitude)
BCC-CSM2-MR	Beijing Climate Center, China Meteorological Administration (China)	160 × 320
CanESM5	Canadian Centre for Climate Modelling and Analysis (Canada)	64 × 128
CNRM-CM6-1	Centre National de Recherches Meteorologiques/Centre Europeen de Recherche et Formation Avancees en Calcul Scientifique (France)	128 × 256
CNRM-ESM2-1	Centre National de Recherches Meteorologiques/Centre Europeen de Recherche et Formation Avancees en Calcul Scientifique (France)	128 × 256
EC-Earth3	EC-EARTH consortium	256 × 512
EC-Earth3-Veg	EC-EARTH consortium	256 × 512
GFDL-CM4	Geophysical Fluid Dynamics Laboratory (United States)	180 × 288
IPSL-CM6A-LR	Institut Pierre Simon Laplace (France)	143 × 144
MPI-ESM1-2-HR	Max Planck Institute for Meteorology (Germany)	192 × 384
MRI-ESM2-0	Meteorological Research Institute (Japan)	160 × 320
NESM3	Nanjing University of Information Science and Technology (China)	96 × 192

23284277, 2022, 10, Downloaded from https://agupubs.onlinelibrary.wiley.com/doi/10.1029/2021EF002378 by Universitetsbiblioteket, Wiley Online Library on [17/11/2022]. See the Terms and Conditions (https://onlinelibrary.wiley.com/terms-and-conditions) on Wiley Online Library for rules of use; OA articles are governed by the applicable Creative Commons License

advantage of eliminating many spurious counts of rainy days in the model. Thus, only a daily precipitation value greater than this threshold is counted as a precipitation (rainfall) event at a given grid point.

The frequency of precipitation (rainfall) event in a given month refers to the total number of days with precipitation (rainfall) in that month. The precipitation (rainfall) intensity refers to the amount of precipitation (rainfall) per unit time (per day in this study), regardless of whether it rains only part of the time (Trenberth et al., 2003). The maximum total precipitation (rainfall) intensity refers to the maximum amount of daily precipitation (rainfall) in a given month. The date of the first rainfall (day number of the year) is used to characterize the onset timing of rainfall events at each grid cell in a given year. The ratio of rainfall day to total precipitation day (RPR) is calculated by dividing the number of days with rainfall by the number of days with total precipitation.

For the experimental design of CMIP5, the beginning of 2006 symbolizes the transition from the historical simulation using the observed forcings to the scenario projections based on the particular representative concentration pathway (RCP) forcings (Wild et al., 2015). Previous studies usually regarded 2006–2015 as a 10-year reference period because this period well represents present-day conditions (Bintanja & Andry, 2017; Müller et al., 2014). Accordingly, we define the future trend for the CMIP5 simulations as the difference in multi-model mean between the periods of 2091–2100 and 2006–2015.

The contribution of local warming to the increase in rainfall days was calculated using the method of Bintanja (2018):

$$\xi = \frac{\Delta f}{\Delta f + (1 - f_0)\,(P_0/P_1 - 1)}$$

where P_0 denotes the number of days with total precipitation over the 2006–2015 period (present day), while P_1 denotes the total precipitation days over the 2091–2100 period (future). The snowfall fraction f is defined as the fraction of the number of days with snowfall to the number of days with total precipitation (P), which is different from that of Bintanja (2018). In that study, f was defined as the ratio of snowfall to total precipitation. $\Delta f = f_1 - f_0$, in which f_0 refers to the average snowfall fraction over the 2006–2015 period (present-day), while f_1 refers to the average snowfall fraction over the 2091–2100 period (future). Δf represents the component of change in rainfall days that can be attributed to temperature change. Accordingly, ξ nonlinearly depends on the background climate state (f_0), climate warming (Δf), and the change in total precipitation (P_0/P_1).

3. Results

3.1. Verification of the Multi-Model Mean Results

Earlier studies demonstrated that the CMIP5 model mean performs a reasonable simulation of Arctic precipitation amount under the strong emission scenario (RCP8.5) (Bintanja & Andry, 2017), and the first 10 years (also the historical reference period in this study) of the simulation have been covered by the current observations. We first conducted the model evaluation in RCP8.5 scenario from 2006 to 2015 based on three reanalysis products (ERA-Interim, ERA5, and MERRA). Figure 1 shows the monthly variations in the number of days with precipitation/rainfall from the CMIP5 multi-model mean and the reanalysis data sets. Various reanalysis data sets consistently show that the number of days with total precipitation is largest in August–September and smallest throughout the spring (Figure 1a), and the number of days with rainfall is largest in July–September and smallest throughout the cold season (November–May) (Figure 1b). The multi-model mean can well reproduce the seasonal cycle and is close to the average value of ERA5 during the same period (Figure 1).

3.2. Projections

3.2.1. Number of Days With Rainfall

In this study, we carried out projections based on CMIP5 simulations driven by the RCP8.5 scenario. As shown in Figure 3c, the projected number of days with rainfall shows an overall increasing trend, indicating that rainfall will occur more frequently in the Arctic. Meanwhile, the extent of rainfall shows a trend of northward expansion, and this trend is observed throughout Arctic Ocean during the warm season (June–October) and most evident in the Atlantic sector during the cold season (November–May) (Figures 3a and 3c). In November–April, the rainfall

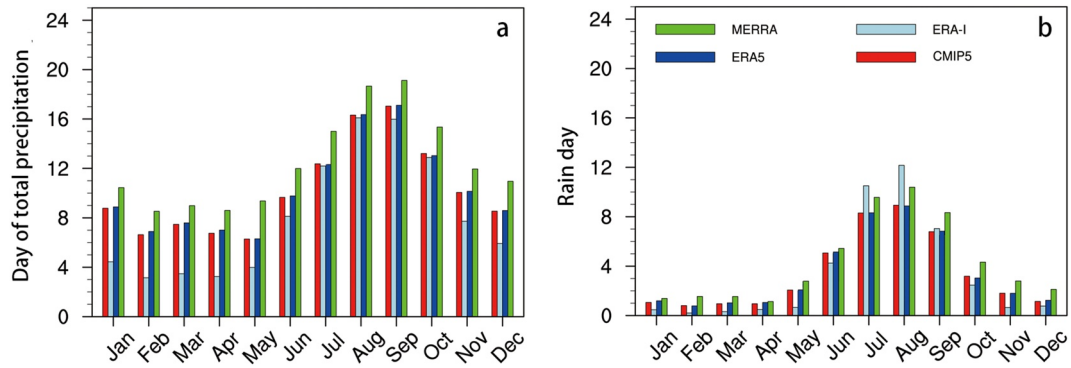

Figure 1. Comparisons between Coupled Model Intercomparison Project Phase 5 multi-model mean and various reanalysis data sets (ERA-Interim, ERA5, and MERRA). (a) The number of days with precipitation averaged over the Arctic (60–90°N) in different months during 2006–2015. (b) Same as in (a) but for the number of days with rainfall. Further analysis indicates that the spatial distribution of Arctic precipitation (rainfall) days could be well reproduced by the multi-model mean in different months, although there are quantitative differences in some areas. There are slight discrepancies in the number of days with total precipitation among different reanalysis data sets, and the magnitude and spatial distribution of total precipitation days from the multi-model mean are closer to those from ERA5 (Figure S1 in Supporting Information S1). The number of days with rainfall from ERA-Interim are less than those from other reanalysis data sets in cold seasons, but more than those from other reanalysis data sets from July to August. The largest diversity of various reanalysis data sets is observed from July to August, and the multi-model mean is between ERA5 and MERRA during this period. In cold seasons (November–April), the rainy days from multi-model mean are less than those from the reanalysis in the Atlantic sector, and closer to that from ERA5 (Figure 2). In summer, the rainy days from ERA-I are more than those from other reanalysis data sets on the Arctic land area, and the multi-model mean is closer to ERA5 and MERRA (Figure 2).

days will increase by up to 12 days/month in the Barents Sea, Greenland Sea, Northern Europe, and Pacific sector by the end of this century as compared with the reference period (2006–2015). During the warm season (June–September), the largest increase in rainfall days will occur over the Arctic Ocean, which can be up to 14 days/month in the central Arctic Ocean in September (Figure 3c). During the transition period of spring-summer (May), the increase mainly occurs over the Arctic land area.

Note that the variability among different models may bring uncertainties to the projections based on the multi-model mean. It can be seen from Figure S2 in Supporting Information S1 that in cold seasons (October–April), the intermodel diversities of the rainy days are mainly observed in the Atlantic and the Pacific sectors, and the highest diversity is found in the Norwegian Sea where the standard deviation of different models can reach 10 days/month. In warm seasons (May–September), the intermodel standard deviations of the rainy days are around 5 days/month in most parts of the Arctic, which are generally lower than those in cold seasons. For the total precipitation days, except for the larger intermodel discrepancies in the Barents Sea in winter, the standard deviations in other parts of the Arctic are around 6 days/month (Figure S3 in Supporting Information S1). To sum up, the multi-model mean of rainy days has larger uncertainty in the Norwegian Sea in cold seasons, and that of total precipitation days has larger uncertainty in the Barents Sea in winter. During other seasons, the intermodel variability is relatively small in the Arctic.

By comparing Figures 3c and 3d, it show that there are large discrepancies in the areas with an increasing trend between the number of days with rainfall and total precipitation, indicating that the more frequent rainfall events in the future are not mainly caused by the increase of total precipitation. We quantitatively estimated the contributions of solid-to-liquid precipitation transition due to local warming and precipitation increases to the increase of rainy days (see the Methods section for details), and the results showed that the local warming contributes more than 90% to the increase in rainy days in March. Even in June when the local warming plays a relatively weak role, it still contributes ~67% of the increase in the number of days with rainfall (Figure 4). On an annual average, the local warming contributes ~83% to the increase in rainy days by the end of this century. In the summer period, the contribution of local warming is smaller than those in other seasons and is mainly observed over the Arctic Ocean (50%–80%) (Figure 5), and the remaining part is contributed by the increase in the number of days with total precipitation. In the cold months (October–April), the local warming contributes to almost all the increases in the number of days with rainfall in the areas where rainfall occurs (Figure 5).

23284277, 2022, 10, Downloaded from https://agupubs.onlinelibrary.wiley.com/doi/10.1029/2021EF002378 by Universitetsbiblioteket, Wiley Online Library on [17/11/2022]. See the Terms and Conditions (https://onlinelibrary.wiley.com/terms-and-conditions) on Wiley Online Library for rules of use; OA articles are governed by the applicable Creative Commons License

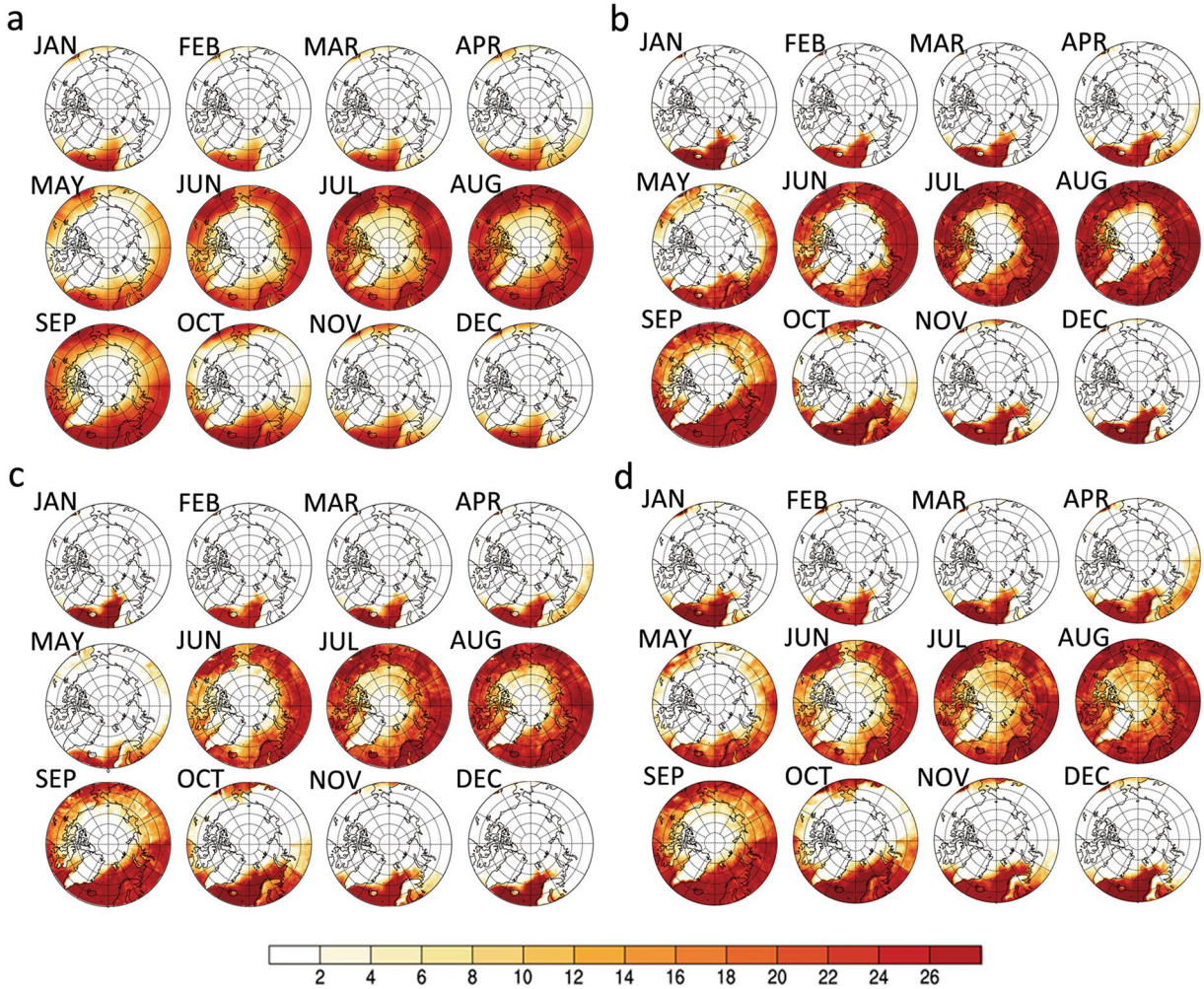

Figure 2. Comparisons of the number of days with rainfall between Coupled Model Intercomparison Project Phase 5 multi-model mean and various reanalysis data sets over the Arctic (60–90°N) in different months for the period 2006–2015. (a) Multi-model mean, (b) ERA-Interim, (c) ERA5, and (d) MERRA.

As shown in Figure 3c, the areas where rainy days increase in the Arctic Ocean are highly consistent with the areas where sea ice retreats. From the above analysis, we know that the increase in rainfall days in the Arctic Ocean is mainly caused by the transition of the precipitation phase due to local warming, manifested in the northward movement of the zero-degree isotherm as the sea ice retreat (Figure S4 in Supporting Information S1). We also noticed that there is also an increase in rainfall days in the Nordic area and the edge of the Greenland Ice Sheet, which may be related to the more frequent and intense intrusion of mid-latitude cyclones (e.g., Webster et al., 2019; Wernli & Papritz, 2018). Such weather systems bring warm and humid air and cause the regional temperature to rise above the melting point, triggering rainfall events (e.g., Binder et al., 2017; Oltmanns et al., 2019; Peeters et al., 2019). This is an important mechanism for increasing rainfall events over the high Arctic.

In the areas at a temperature close to the melting point, the changes in the precipitation phase are particularly sensitive to local warming (Figure S4 in Supporting Information S1). With climate warming, rainfall events are observed in these areas by the end of this century, and the frequency of rainfall events has an increasing trend (Figure 3c). This phenomenon is particularly evident in the Arctic Ocean in August and September. In contrast, the local warming is not enough to raise the temperature above the melting point in parts of Siberia during the cold seasons (Figure S4 in Supporting Information S1). Therefore, even under the highest emission scenario, there is no significant change in the number of days with rainfall in this region by the end of this century (Figure 3c).

23284277, 2022, 10, Downloaded from https://agupubs.onlinelibrary.wiley.com/doi/10.1029/2021EF002378 by Universiteitsbibliotheek, Wiley Online Library on [17/11/2022]. See the Terms and Conditions (https://onlinelibrary.wiley.com/terms-and-conditions) on Wiley Online Library for rules of use; OA articles are governed by the applicable Creative Commons License

10.1029/2021EF002378

23284277, 2022, 10, Downloaded from https://agupubs.onlinelibrary.wiley.com/doi/10.1029/2021EF002378 by Universitetsbiblioteket, Wiley Online Library on [17/11/2022]. See the Terms and Conditions (https://onlinelibrary.wiley.com/terms-and-conditions) on Wiley Online Library for rules of use; OA articles are governed by the applicable Creative Commons License

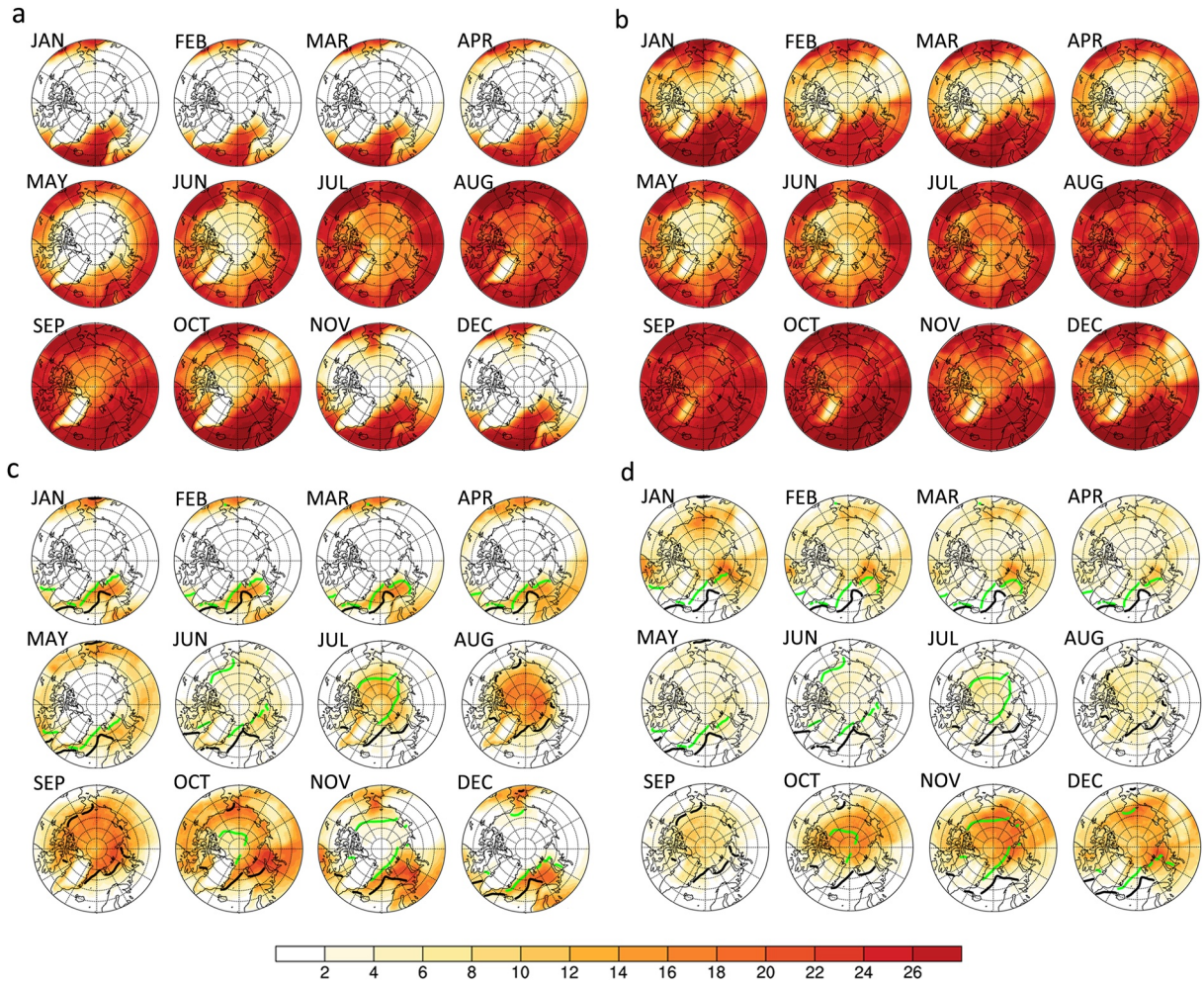

Figure 3. Projected number of days with rainfall and total precipitation over the Arctic for each month. (a) The number of days with rainfall averaged from 2091 to 2100. (b) The number of days with total precipitation averaged from 2091 to 2100. The difference in the number of days with (c) rainfall and (d) total precipitation from the present-day climate (2006–2015). The present-day sea ice extent (black solid line) and the projected sea ice extent (green solid line) are shown in panels (c and d). The sea ice extent is defined as the area with an ice concentration greater than 15%.

3.2.2. Long-Term Trends of Rainfall Days

The projections further show that the largest increase in the number of days with rainfall is observed in August–October (Figure 4), corresponding to the period with the largest increase in the RPR (Figure 6f), while the largest increase in the number of days with total precipitation is found in the cold seasons (October–May) (Figure 6d). This further confirms that the increase in rainy days is dominated by the increasing RPR (i.e., solid-to-liquid precipitation transition). Air temperature in September is slightly lower than the melting point during the reference period. Thus, the precipitation phase in this period is extremely sensitive to the temperature rise. The projections show that the RPR increases by ~40% due to the strong local warming with the rapid sea ice retreat in September by the end of this century. As a result, the rainy days increase by 11 days/month during the same period (Figure 6b).

As shown in Figure 6c, the number of days with total precipitation is highest in August under the present-day climate; however, starting in the middle of this century, September has become the month with the most frequent precipitation events. It can be seen from Figure 3c that the Arctic Ocean becomes ice-free during August and September at the end of this century under the strong emission scenario, which provides abundant water vapor, making September the month with the most frequent precipitation from the middle of this century. Meanwhile, severe local warming occurs during the ice-free period (Figure S4 in Supporting Information S1), leading to a great increase in the RPR in the Arctic (Figure 6f). Consequently, August will replace July as the month with

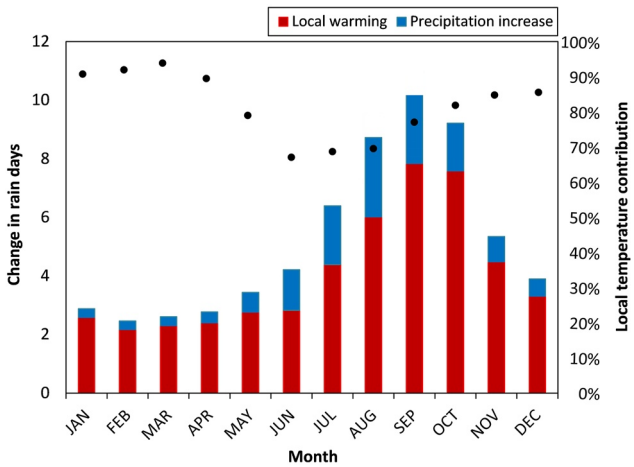

Figure 4. The projected Arctic mean (60–90°N) increases in the number of days with rainfall compared with the present day, including the contributions of changes in local temperature and total precipitation. Black dots indicate the percentage by which local warming determines the increase in rainfall days.

the highest RPR in the second half of this century (89% by the end of this century) (Figure 6e), resulting in the most frequent rainfall events in August (Figure 6a).

3.2.3. Timing of the First Rainfall

The occurrence of rainfall events in spring is an important indicator of the onset of the Arctic ablation period, and it can initiate and accelerate the melting of sea ice and snow cover in the Arctic (e.g., Dou et al., 2019; Landrum & Holland, 2020). The projections show that the timing of the first rainfall event in spring will be earlier than the present day by ~38 days on average across the Arctic by the end of this century. The shift in the early melt season rainfall is most evident in the Pacific and North Atlantic sectors, especially in the Chukchi Sea and the Northern Barents Sea, where the onset date of rainfall event in spring occurs ~3 months (one season) earlier than that of the present day (Figure 7). This means that spring rainfall will occur much earlier in most parts of the Arctic at the end of this century, and the expanded rain season will have a profound impact on the local climate change and ice and snow environment in the Arctic.

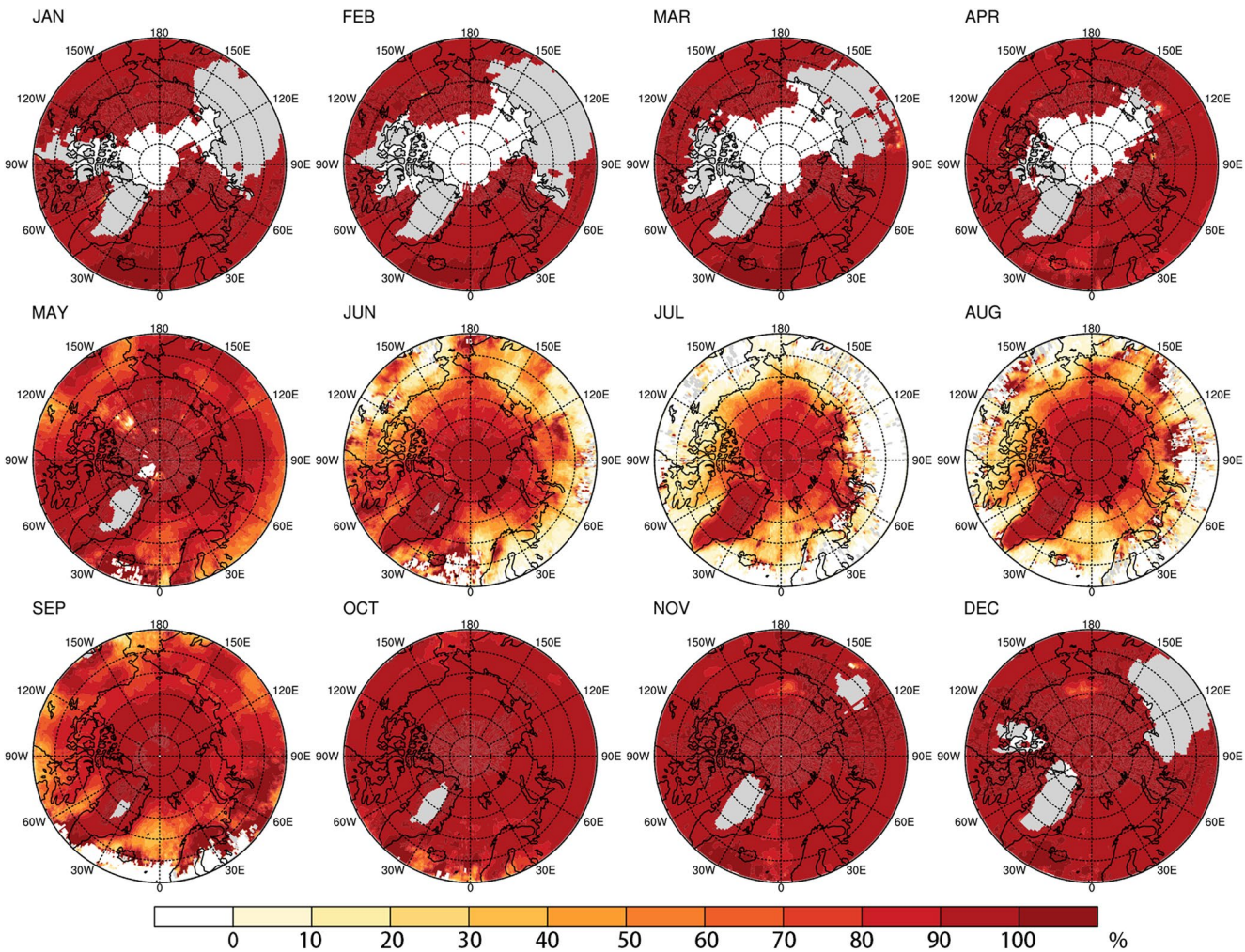

Figure 5. The projected increase in the number of days with rainfall in the Arctic was attributed to local warming; 100% means that the increase in rainfall days is completely caused by local warming. The gray shadows indicate areas where no rainfall occurs.

23284277, 2022, 10, Downloaded from https://agupubs.onlinelibrary.wiley.com/doi/10.1029/2021EF002378 by Universiteitsbibliotheek, Wiley Online Library on [17/11/2022]. See the Terms and Conditions (https://onlinelibrary.wiley.com/terms-and-conditions) on Wiley Online Library for rules of use; OA articles are governed by the applicable Creative Commons License

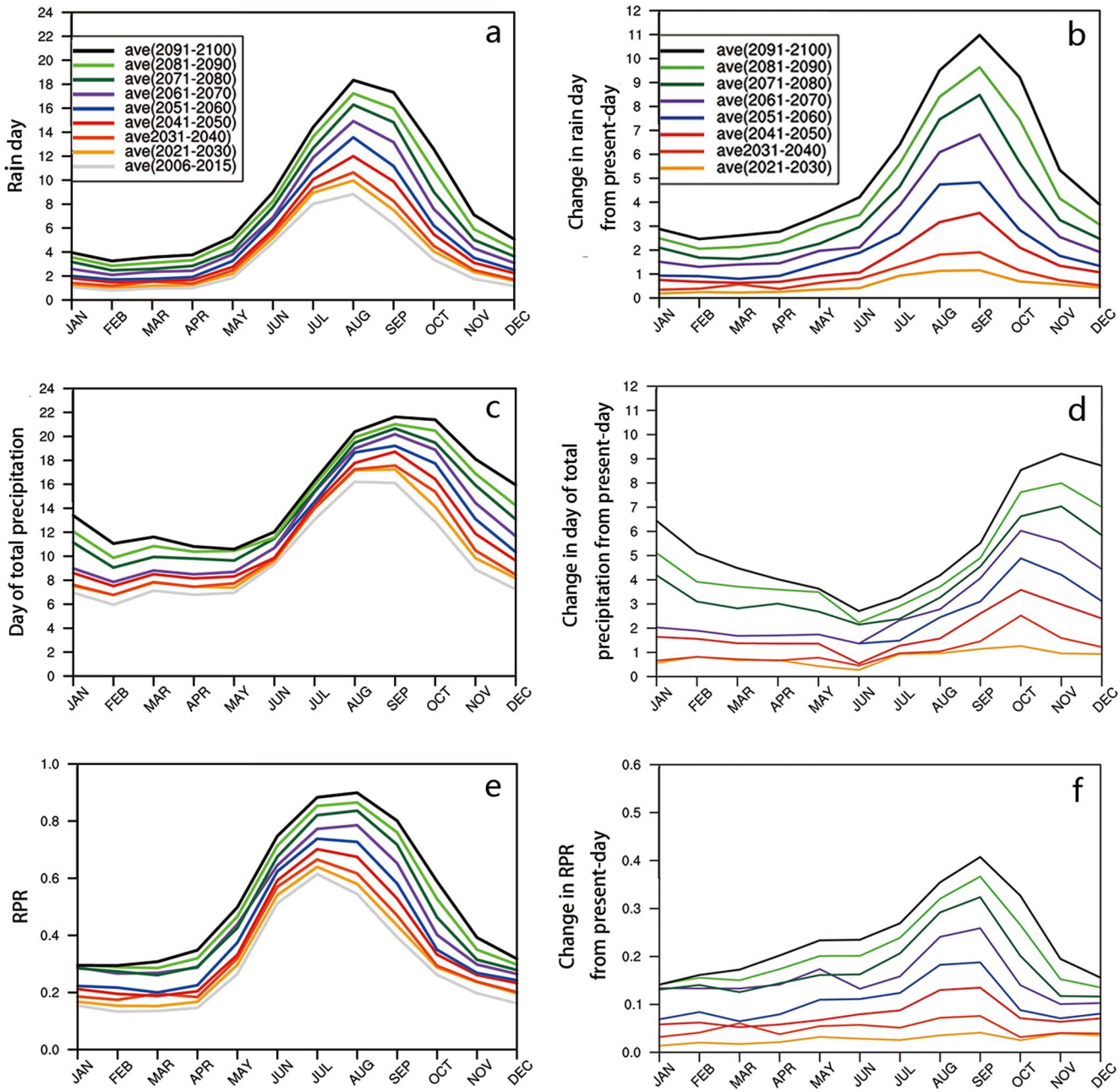

Figure 6. Variations in the 10-year average of the number of days with rainfall and total precipitation and their ratio averaged in the Arctic (60–90°N) from 2006 to 2100. (a) The number of days with rainfall. (b) Changes in the number of rainy days from the present day (2006–2015). (c) The number of days with total precipitation. (d) Changes in the precipitation days from the present day. (e) The ratio of rainy days to total precipitation days (RPR). (f) Changes in RPR from the present day.

3.2.4. Intensity of Rainfall

The intensity of rainfall also shows an overall increasing trend in the future (Figure 8). By the end of this century, the intensity of the warm season (June–September) rainfall can reach greater than 6 mm/day over the Arctic continent, which is stronger than the intensity of rainfall (~4 mm/day in average) in the Arctic Ocean during the same period. In the winter part of the year (October–April), rainfall events only occur in the Pacific and Atlantic sectors with intensities greater than 3 mm/day (Figure 8a).

From June to September, the projected increase in rainfall intensity can be up to ~2 mm/day over parts of the Arctic land area, including western and southern Greenland, which is larger than the increase over the Arctic

23284277, 2022, 10, Downloaded from https://agupubs.onlinelibrary.wiley.com/doi/10.1029/2021EF002378 by Universiteitsbibliotheek, Wiley Online Library on [17/11/2022]. See the Terms and Conditions (https://onlinelibrary.wiley.com/terms-and-conditions) on Wiley Online Library for rules of use; OA articles are governed by the applicable Creative Commons License

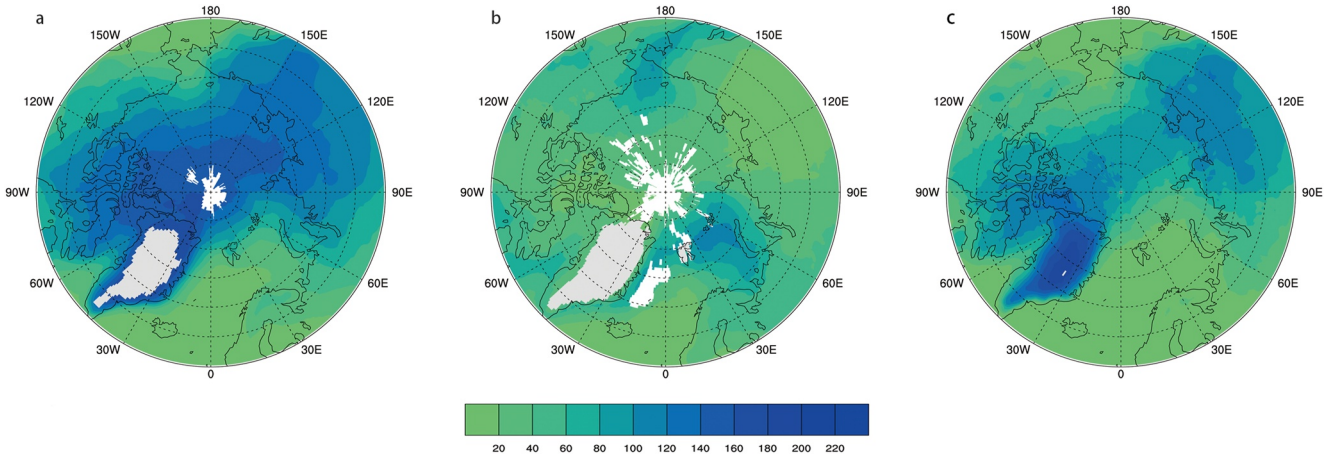

Figure 7. Projections of the first rainfall date in the Arctic during 2091–2100 for the high-emission scenario forcing based on the multi-model mean results of Coupled Model Intercomparison Project Phase 5 (CMIP5) (RCP8.5) and CMIP6 (SSP585). (a) CMIP5 model mean. (b) Differences in the projected timing of the first rainfall from the present day based on the CMIP5 model mean. (c) CMIP6 model mean.

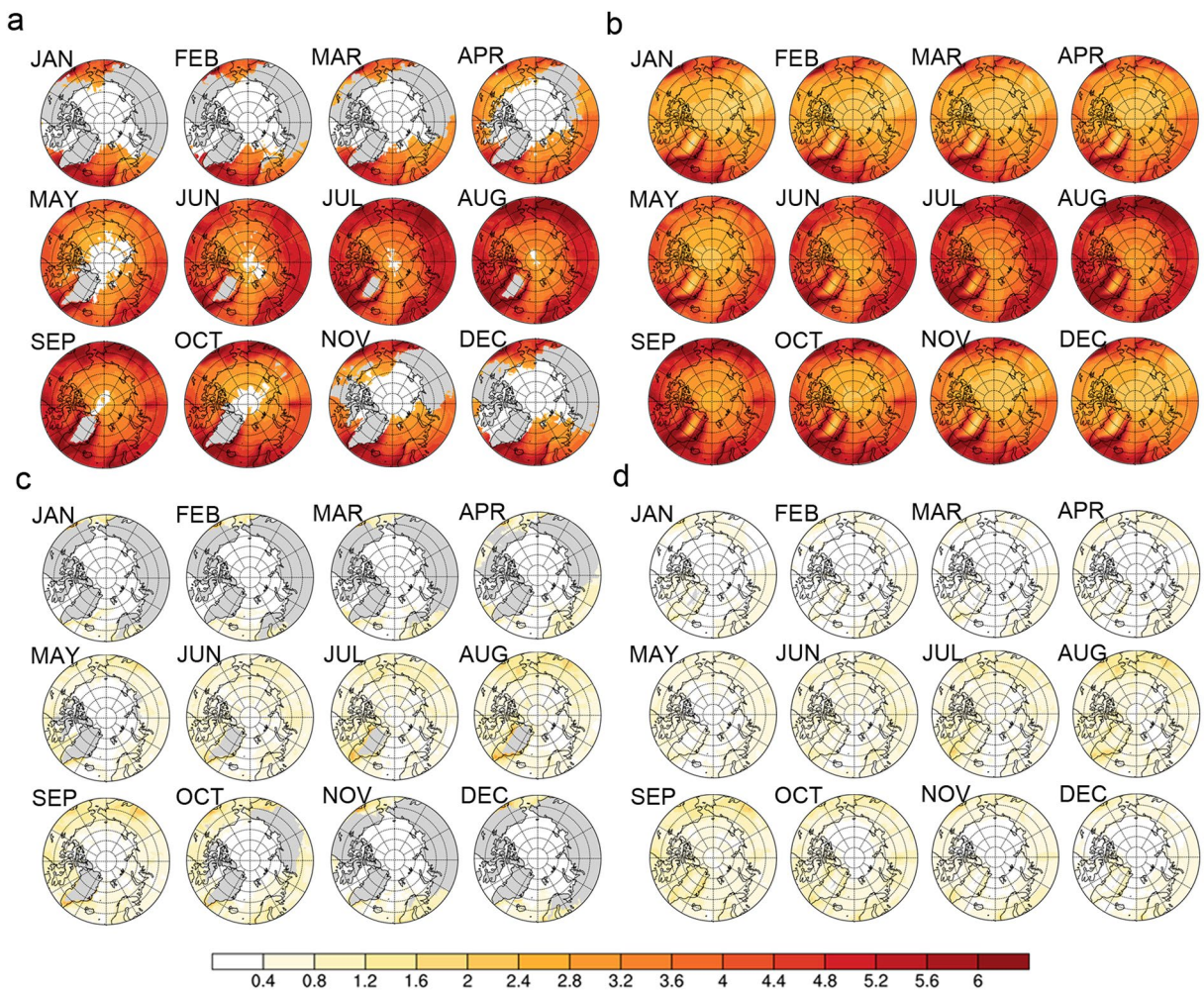

Figure 8. Same as in Figure 3 but for the intensities of rainfall and total precipitation events during 2091–2100 (unit: mm/day). (a) Rainfall intensity. (b) Intensity of total precipitation. (c) Differences in the projected rainfall intensity from the present day. (d) Differences in the projected intensity of total precipitation from the present day.

23284277, 2022, 10, Downloaded from https://agupubs.onlinelibrary.wiley.com/doi/10.1029/2021EF002378 by Universiteitsbibliotheek, Wiley Online Library on [17/11/2022]. See the Terms and Conditions (https://onlinelibrary.wiley.com/terms-and-conditions) on Wiley Online Library for rules of use; OA articles are governed by the applicable Creative Commons License

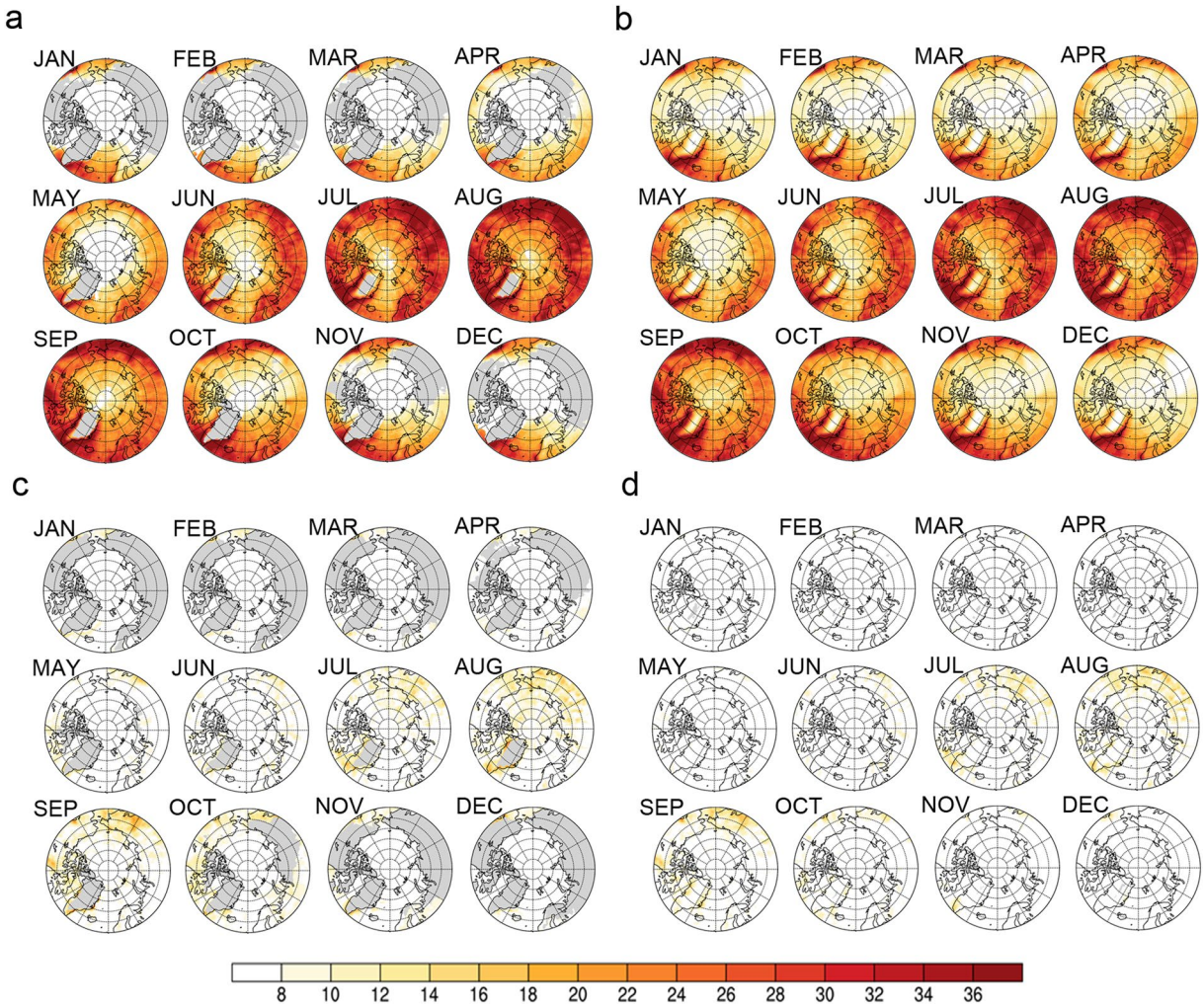

Figure 9. Projected monthly (a) maximum intensity of rainfall and (b) the maximum intensity of total precipitation in the Arctic from the Coupled Model Intercomparison Project Phase 5 multi-model mean. The differences in the projected maximum intensity of (c) rainfall and (d) total precipitation from the present day (unit: mm/day).

Ocean (~0.5 mm/day), indicating that the response of rainfall intensity to the climate change is more sensitive over the Arctic land area in the warm season. The earlier studies based on CMIP5 projections suggested that the warm season moisture inflow from the lower latitudes will increase significantly at the end of this century under high-emission scenarios (Bintanja & Selten, 2014), leading to a larger increase in the intensity of rainfall events on the land area since the frequencies of rainfall events will not increase during the same period (Figure 3c). Moreover, the increase in rainfall intensity is mainly observed over the lower latitudes of the Pacific and Atlantic sectors during the winter part of the year because it is still too cold to form rainfall during this period in other regions by the end of this century (Figure 8c).

We further analyzed the projections of the maximum intensity of rainfall, and the results indicate that the maximum intensity of rainfall in summer (June–September) is significantly higher than those in other seasons over the Arctic continent (Figure 9a). The strongest rainfall events are likely to be observed over northwest Alaska, eastern Siberia, northern Europe, and the marginal area of Greenland in the future, and the intensity of these rainfall events can reach 32 mm/day (Figure 9a). In large parts of eastern Siberia, the increase of the maximum intensity of rainfall events in summer will be larger than 10 mm/day relative to the present day, demonstrating that the Arctic region may suffer more heavy rainfall events during the warm season with global warming. In the cold

23284277, 2022, 10, Downloaded from https://agupubs.onlinelibrary.wiley.com/doi/10.1029/2021EF002378 by Universiteitsbibliotheek, Wiley Online Library on [17/11/2022]. See the Terms and Conditions (https://onlinelibrary.wiley.com/terms-and-conditions) on Wiley Online Library for rules of use; OA articles are governed by the applicable Creative Commons License

months (November–April), the maximum intensity of rainfall events will not change significantly in the Arctic except for a slight increase over the Pacific sector (Figure 9c).

4. Discussion and Conclusions

In this study, based on the CMIP5 projections, the changes in Arctic rainfall events in the future are evaluated under the high-emission scenario (RCP8.5). The results show that the frequency and intensity of rainfall events both show an increasing trend in the Arctic. The increasing trend of the number of days with rainfall is mainly observed in the Atlantic and Pacific sectors in the cold seasons, while it is mainly observed over the Arctic Ocean in the warm seasons, especially in September. The increase of rainfall days in the Arctic is mainly determined by the local warming and the sensitivity of the precipitation phase to the temperature rise. These two factors together result in the spatial differences of the increasing trends of rainfall days in the Arctic during various seasons.

In the cold seasons, the local warming in the Atlantic sector contributes most to the increase in rainfall days (~90%) over the Arctic Ocean. In summer, the contribution of local warming is relatively small (~70%) and mainly reflected over the Arctic Ocean, and the remaining part was contributed by the increase in total precipitation. The sharp retreat of sea ice in summer leads to an increase in local water vapor and hence more precipitation (Bintanja & Selten, 2014) that occurs mainly in liquid form over the Arctic Ocean in September. Note that, in addition to the increase in the frequency and intensity of rainfall, we found that the first rainfall at the end of this century occurred earlier than the present day by ~38 days on average over the Arctic, and the largest changes are observed over the Pacific and Atlantic sectors, which means that the ice ablation period will be further prolonged in the Arctic under the high-emission scenario.

The increase of rainfall intensity is mainly manifested in the Pacific and Atlantic sectors during the cold seasons (November–April), while it is observed in most parts of the Arctic during the warm seasons (May–September), and the largest increase up to 2 mm/day is observed in large part of the Arctic continent. The intensified rainfall events in the lower latitudes of the Arctic in the future are mainly caused by the increased transport of water vapor from low latitudes to the Pole. The largest increase in the maximum intensity of rainfall occurs over eastern Siberia, western Alaska and the southwestern edge of Greenland from July to September, which can reach ~12 mm/day. This means that there will be more heavy rainfall events in the warm season in a large part of the Arctic land area with global warming.

We further examined the projections of Arctic rainfall based on the latest phase of CMIP (CMIP6) models (see Table 2). As shown in Figure 10 and Figure S5 in Supporting Information S1, the two-phase multi-model means are highly consistent in simulating the seasonal cycle of air temperature, frequency and intensity of rainfall in the Arctic, although different models are selected in these two phases of CMIP. In general, CMIP6 models simulate a slightly larger amount of total precipitation (rainfall), which is reflected both in the intensity and frequency of precipitation (rainfall) events. The differences in the two-phase model mean in the number of days with total precipitation, and the amount of total precipitation are mainly led to by the differences in rainy days and rainfall amount, which are basically caused by the warmer climate in the average result of the selected CMIP6 models in this study (Figure 10a). For the same reason, the timing of first rainfall projected by CMIP6 is slightly earlier than that by CMIP5 over the Pacific and Atlantic sectors (Figures 7a and 7c). Despite the above differences, it can be concluded that the projections of CMIP6 broadly support the results of more frequent and intense rainfall events in the Arctic than those derived from CMIP5.

Additionally, the projections show the rainfall events tend to advance toward the center of the Arctic Ocean and inland area of the Greenland Ice Sheet in August in the future (Figure S5 in Supporting Information S1 and Figure 7c). In view of the boosting effects of rainfall on snow and ice ablation (Dou et al., 2019; Landrum & Holland, 2020; Neumann et al., 2019; Oltmanns et al., 2019), rainfall will become an important factor in accelerating the mass loss of snow cover, sea ice and ice sheet in a rapid warming Arctic under the background of global warming.

23284277, 2022, 10, Downloaded from https://agupubs.onlinelibrary.wiley.com/doi/10.1029/2021EF002378 by Universiteitsbibliotheek, Wiley Online Library on [17/11/2022]. See the Terms and Conditions (https://onlinelibrary.wiley.com/terms-and-conditions) on Wiley Online Library for rules of use; OA articles are governed by the applicable Creative Commons License

10.1029/2021EF002378

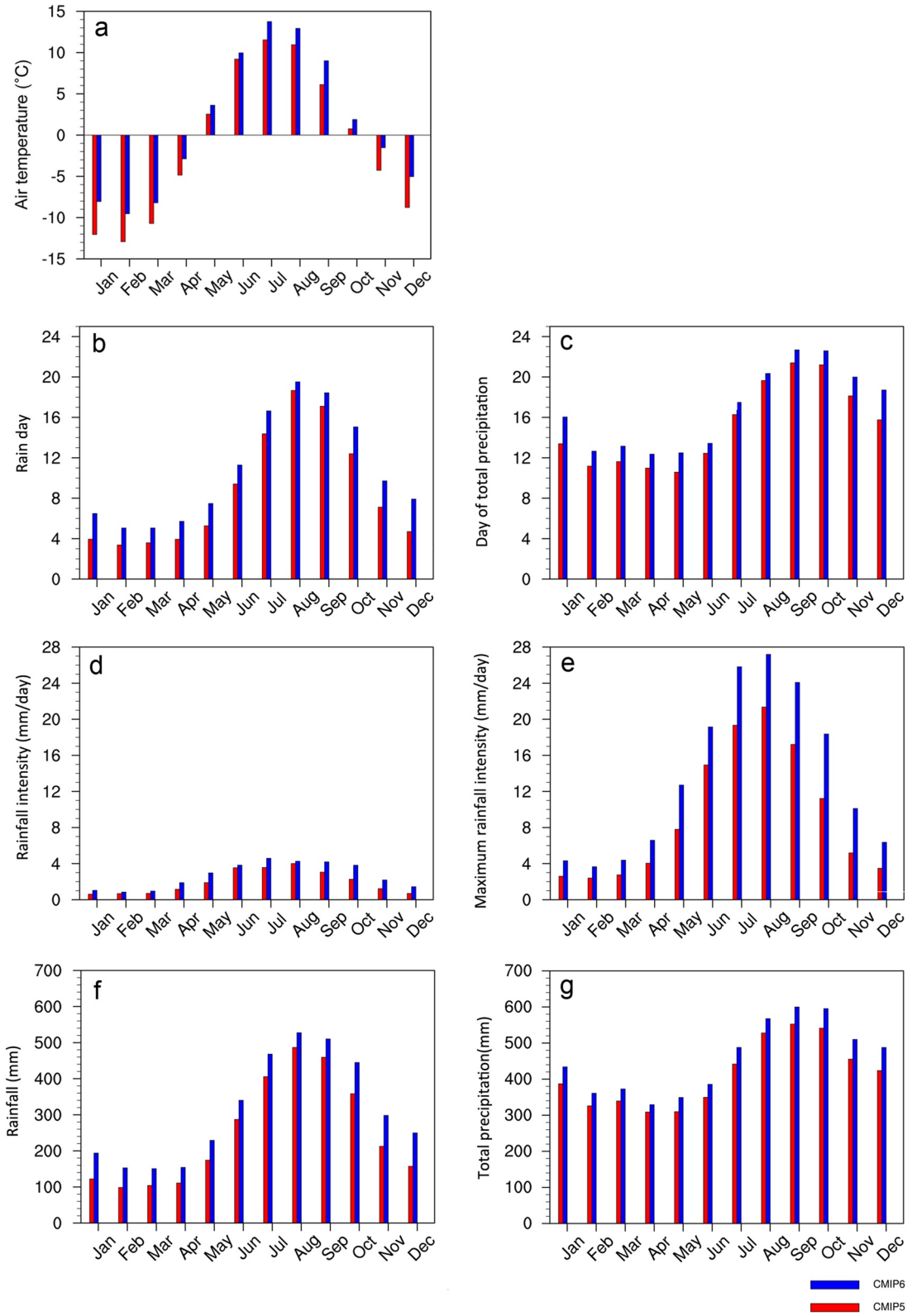

Figure 10. Comparisons of the projections between two phases of the CMIP model means under their high-emission scenarios during 2091–2100. (a) Air temperature. (b) The number of days with rainfall. (c) The number of days with total precipitation. (d) Rainfall intensity. (e) Maximum intensity of rainfall. (f) Rainfall amount. (g) Amount of total precipitation.

23284277, 2022, 10, Downloaded from https://agupubs.onlinelibrary.wiley.com/doi/10.1029/2021EF002378 by Universiteitsbibliotheek, Wiley Online Library on [17/11/2022]. See the Terms and Conditions (https://onlinelibrary.wiley.com/terms-and-conditions) on Wiley Online Library for rules of use; OA articles are governed by the applicable Creative Commons License

Data Availability Statement

Reanalyzes files for ERA-Interim are available from https://apps.ecmwf.int/datasets/data/interim-full-daily/levtype=sfc/. Reanalyzes files for ERA5 are obtained from the Copernicus Climate Change Service (C3S) Climate Date Store (https://cds.climate.copernicus.eu/cdsapp%23/dataset/reanalysis%2Dera5%2Dsingle%2Dlevelsmonthlymeans%3Ftab%3Dform). Reanalyzes files for MERRA are available from the NASA Goddard Earth Sciences (GES) Data and Information Services Center (DISC) (https://disc.sci.gsfc.nasa.gov/datasets?page=1%26keywords=merra). The CMIP5 and CMIP6 outputs can be downloaded from the Earth System Grid Federation (https://esgf-node.llnl.gov/search/cmip6/ and https://esgf-node.llnl.gov/search/cmip5/).

Acknowledgments
We wish to acknowledge ECMWF for ERA-Interim and ERA5 data, and acknowledge NASA GES-DISC for MERRA data. This study is funded by the National Key Research and Development Program of China (2018YFC1406104) and the National Natural Science Foundation of China (NSFC 42222608, 41971084).

References

Binder, H., Boettcher, M., Grams, C. M., Joos, H., Pfahl, S., & Wernli, H. (2017). Exceptional air mass transport and dynamical drivers of an extreme wintertime Arctic warm event. *Geophysical Research Letters*, *44*(23), 12028–12036. https://doi.org/10.1002/2017GL075841

Bintanja, R. (2018). The impact of Arctic warming on increased rainfall. *Scientific Reports*, *8*(1), 16001. https://doi.org/10.1038/s41598-018-34450-3

Bintanja, R., & Andry, O. (2017). Towards a rain-dominated Arctic. *Nature Climate Change*, *7*(4), 263–267. https://doi.org/10.1038/nclimate3240

Bintanja, R., & Selten, F. M. (2014). Future increases in Arctic precipitation linked to local evaporation and sea-ice retreat. *Nature*, *509*(7501), 479–482. https://doi.org/10.1038/nature13259

Bintanja, R., van der Wiel, K., van der Linden, E. C., Reusen, J., Bogerd, L., Krikken, F., & Selten, F. M. (2020). Strong future increases in Arctic precipitation variability linked to poleward moisture transport. *Science Advances*, *6*(7), eaax6869. https://doi.org/10.1126/sciadv.aax6869

Boer, G. J. (2009). Changes in interannual variability and decadal potential predictability under global warming. *Journal of Climate*, *22*(11), 3098–3109. https://doi.org/10.1175/2008jcli2835.1

Bring, A., Fedorova, I., Dibike, Y., Hinzman, L., Mård, J., Mernild, S. H., et al. (2016). Arctic terrestrial hydrology: A synthesis of processes, regional effects, and research challenges. *Journal of Geophysical Research: Biogeosciences*, *121*(3), 621–649. https://doi.org/10.1002/2015JG003131

Cohen, J., Ye, H., & Jones, J. (2015). Trends and variability in rain-on-snow events. *Geophysical Research Letters*, *42*(17), 7115–7122. https://doi.org/10.1002/2015GL065320

Davies, F. J., Renssen, H., & Goosse, H. (2014). The Arctic freshwater cycle during a naturally and an anthropogenically induced warm climate. *Climate Dynamics*, *42*(7–8), 2099–2112. https://doi.org/10.1007/s00382-013-1849-y

Dou, T., Xiao, C., Liu, J., Han, W., Du, Z., Mahoney, A. R., et al. (2019). A key factor initiating surface ablation of Arctic sea ice: Earlier and increasing liquid precipitation. *The Cryosphere*, *13*(4), 1233–1246. https://doi.org/10.5194/tc-13-1233-2019

Dou, T., Xiao, C., Liu, J., Wang, Q., Pan, S., Su, J., et al. (2021). Trends and spatial variation in rain-on-snow events over the Arctic Ocean during the early melt season. *The Cryosphere*, *15*(2), 883–895. https://doi.org/10.5194/tc-15-883-2021

Forbes, B. C., Kumpula, T., Meschtyb, N., Laptander, R., Macias-Fauria, M., Zetterberg, P., et al. (2016). Sea ice, rain-on-snow and tundra reindeer nomadism in Arctic Russia. *Biology Letters*, *12*(11), 20160466. https://doi.org/10.1098/rsbl.2016.0466

Kattsov, V. M., & Walsh, J. E. (2000). Twentieth-century trends of Arctic precipitation from observational data and a climate model simulation. *Journal of Climate*, *13*(8), 1362–1370. https://doi.org/10.1175/1520-0442(2000)013<1362:tctoap>2.0.co;2

Landrum, L., & Holland, M. M. (2020). Extremes become routine in an emerging new Arctic. *Nature Climate Change*, *10*(12), 1108–1115. https://doi.org/10.1038/s41558-020-0892-z

Lopez, P. (2007). Cloud and precipitation parameterizations in modeling and variational data assimilation: A review. *Journal of the Atmospheric Sciences*, *64*(11), 3766–3784. https://doi.org/10.1175/2006jas2030.1

Müller, B., Wild, M., Driesse, A., & Behrens, K. (2014). Rethinking solar resource assessments in the context of global dimming and brightening. *Solar Energy*, *99*, 272–282. https://doi.org/10.1016/j.solener.2013.11.013

Neumann, R. B., Moorberg, C. J., Lundquist, J. D., Turner, J. C., Waldrop, M. P., McFarland, J. W., et al. (2019). Warming effects of spring rainfall increase methane emissions from thawing permafrost. *Geophysical Research Letters*, *46*(3), 1393–1401. https://doi.org/10.1029/2018gl081274

Oltmanns, M., Straneo, F., & Tedesco, M. (2019). Increased Greenland melt triggered by large-scale, year-round cyclonic moisture intrusions. *The Cryosphere*, *13*(3), 815–825. https://doi.org/10.5194/tc-13-815-2019

Pan, S., Dou, T., Lin, L., Yang, J., Zhang, F., Duan, M., et al. (2020). Larger sensitivity of Arctic precipitation phase to aerosol than greenhouse gas forcing. *Geophysical Research Letters*, *47*, 23. https://doi.org/10.1029/2020GL090452

Peeters, B., Pedersen, Å. Ø., Loe, L. E., Isaksen, K., Veiberg, V., Stien, A., et al. (2019). Spatiotemporal patterns of rain-on-snow and basal ice in high Arctic Svalbard: Detection of a climate-cryosphere regime shift. *Environmental Research Letters*, *14*(1), 015002. https://doi.org/10.1088/1748-9326/aaefb3

Perovich, D., Polashenski, C., Arntsen, A., & Stwertka, C. (2017). Anatomy of a late spring snowfall on sea ice. *Geophysical Research Letters*, *44*(6), 2802–2809. https://doi.org/10.1002/2016GL071470

Qian, T., Dai, A., Trenberth, K. E., & Oleson, K. W. (2006). Simulation of global land surface conditions from 1948 to 2004. Part I: Forcing data and evaluations. *Journal of Hydrometeorology*, *7*(5), 953–975. https://doi.org/10.1175/JHM540.1

Screen, J. A., & Simmonds, I. (2012). Declining summer snowfall in the Arctic: Causes, impacts and feedbacks. *Climate Dynamics*, *38*(11–12), 2243–2256. https://doi.org/10.1007/s00382-011-1105-2

Shepherd, A., Ivins, E., Rignot, E., Smith, B., van den Broeke, M., Velicogna, I., et al. (2019). Mass balance of the Greenland ice sheet from 1992 to 2018. *Nature*, *579*(7798), 233–239. https://doi.org/10.1038/s41586-019-1855-2

Trenberth, K. E. (2011). Changes in precipitation with climate change. *Climate Research*, *47*(1), 123–138. https://doi.org/10.3354/cr00953

Trenberth, K. E., Dai, A., Rasmussen, R. M., & Parsons, D. B. (2003). The changing character of precipitation. *Bulletin America Meteorology Social*, *84*(9), 1205–1217. https://doi.org/10.1175/BAMS-84-9-1205

Vihma, T., Screen, J., Tjernström, M., Newton, B., Zhang, X., Popova, V., et al. (2016). The atmospheric role in the Arctic water cycle: A review on processes, past and future changes, and their impacts. *Journal of Geophysical Research: Biogeosciences*, *121*(3), 586–620. https://doi.org/10.1002/2015JG003132

Webster, M. A., Parker, C., Boisvert, L., & Kwok, R. (2019). The role of cyclone activity in snow accumulation on Arctic sea ice. *Nature Communications*, *10*(1), 1–12. https://doi.org/10.1038/s41467-019-13299-8

23284277, 2022, 10, Downloaded from https://agupubs.onlinelibrary.wiley.com/doi/10.1029/2021EF002378 by Universiteitsbibliotheek, Wiley Online Library on [17/11/2022]. See the Terms and Conditions (https://onlinelibrary.wiley.com/terms-and-conditions) on Wiley Online Library for rules of use; OA articles are governed by the applicable Creative Commons License

Wernli, H., & Papritz, L. (2018). Role of polar anticyclones and mid-latitude cyclones for Arctic summertime sea-ice melting. *Nature Geoscience*, *11*(2), 108–113. https://doi.org/10.1038/s41561-017-0041-0

Wild, M., Folini, D., Henschel, F., Fischer, N., & Mueller, B. (2015). Projections of long-term changes in solar radiation based on CMIP5 climate models and their influence on energy yields of photovoltaic systems. *Solar Energy*, *116*, 12–24. https://doi.org/10.1016/j.solener.2015.03.039

Wrona, F. J., Johansson, M., Culp, J. M., Jenkins, A., Mård, J., Myers-Smith, I. H., et al. (2016). Transitions in Arctic ecosystems: Ecological implications of a changing hydrological regime. *Journal of Geophysical Research: Biogeosciences*, *121*(3), 650–674. https://doi.org/10.1002/2015JG003133

Zhang, X., He, J., Zhang, J., Polyakov, I., Gerdes, R., Inoue, J., & Wu, P. (2013). Enhanced poleward moisture transport and amplified northern high-latitude wetting trend. *Nature Climate Change*, *3*(1), 47–51. https://doi.org/10.1038/nclimate1631

23284277, 2022, 10, Downloaded from https://agupubs.onlinelibrary.wiley.com/doi/10.1029/2021EF002378 by Universiteitsbibliotheek, Wiley Online Library on [17/11/2022]. See the Terms and Conditions (https://onlinelibrary.wiley.com/terms-and-conditions) on Wiley Online Library for rules of use; OA articles are governed by the applicable Creative Commons License